



This is a self-archived version of an original article. This version may differ from the original in pagination and typographic details.

Author(s): Virtanen, P.; Braggio, A.; Giazotto, F.

Title: Superconducting size effect in thin films under electric field: Mean-field self-consistent model

Year: 2019

Version: Published version

Copyright: © 2019 American Physical Society

Rights: In Copyright

Rights url: <http://rightsstatements.org/page/InC/1.0/?language=en>

Please cite the original version:

Virtanen, P., Braggio, A., & Giazotto, F. (2019). Superconducting size effect in thin films under electric field: Mean-field self-consistent model. *Physical Review B*, 100(22), Article 224506.
<https://doi.org/10.1103/PhysRevB.100.224506>

Superconducting size effect in thin films under electric field: Mean-field self-consistent model

P. Virtanen[✉], A. Braggio, and F. Giazotto

NEST, Istituto Nanoscienze-CNR and Scuola Normale Superiore, I-56127 Pisa, Italy



(Received 11 March 2019; revised manuscript received 6 November 2019; published 9 December 2019)

We consider the effects of an externally applied electrostatic field on superconductivity, self-consistently within a BCS mean-field model, for a clean three-dimensional (3D) metal thin film. The electrostatic change in superconducting condensation energy scales as Δ/μ close to subband edges as a function of the Fermi energy μ and follows 3D scaling (Δ/μ)² away from them. We discuss nonlinearities beyond the gate effect and contrast results with recent experiments on gating effects on Josephson junctions.

DOI: [10.1103/PhysRevB.100.224506](https://doi.org/10.1103/PhysRevB.100.224506)

I. INTRODUCTION

Quantum oscillations in superconducting properties due to size quantization in thin films were predicted early [1–4], and they were later observed in metallic films [5–8]. Modification of superconducting properties by changing the electron density by electrostatic fields was also observed [9–14] and is best studied in high- T_c superconductors where the charge density can be low enough to enable efficient gating. Generally, modifications of the critical temperature T_c and critical current I_c have been reported. Modification of I_c only was also recently reported in Refs. [14,15] in metallic thin-film samples, but the proper interpretation in the latter is still unclear.

Electrostatics of superconductors is an old problem (see, e.g., Ref. [16] for a historical review), and the effect of electric fields on superconducting surfaces were theoretically discussed in several works [17–24]. In these works, effects on the amplitude of superconductivity (T_c) are usually related to modulation of the electronic density of states (DOS), which is also what contributes to the quantum size effects. A common approach is to consider “surface doping” and assume the DOS is modified within a Thomas-Fermi screening length from the surface. Self-consistently screened calculations in superconductors were previously discussed in Refs. [25–27] in a different context. For the normal state, there is a large body of literature on microscopic calculations with surface screening, which are routine today, e.g., using density functional theory [24,28]. Modification of I_c , on the other hand, is often assumed to come from changes in the vortex surface pinning potential [14,29].

In a simple picture, a static electric field appears as a perturbation of the potential that confines electrons within the thin film. Static perturbations generally extend up to a screening length from the surface, so their effect decreases towards high charge density. Although the effects increase with the applied electric field, achievable field magnitude is limited by electric breakdown (e.g., via field emission [30]).

Electrostatic gating of superconductivity in the BCS mean-field picture relies on electron-hole asymmetry within an

energy window determined by the order parameter and Debye frequency centered at the Fermi level [31–34]. In a simple, clean thin-film model, strong asymmetry naturally exists in the form of the steplike multiband two-dimensional (2D) DOS, which also gives rise to the quantum size effect, and the picture also extends to weakly disordered samples. The only questions are to what degree the DOS asymmetry is retained, even though sharp features in the DOS are smeared by disorder [35], and when samples cannot be significantly gated (metallic regime such as in Ref. [15]) since the Fermi level is not necessarily fixed at a sensitive point. Regardless, sharp DOS features can increase the charge density range in which electrostatic effects are large enough to be observed. However, few explicit results on the interplay between the surface field and the size effects in the high charge density regime seem to have appeared in the literature. Motivated by the recent experimental results [15] where large effects were seen, we revisit the problem.

In this work, we write down and solve a simple mean-field model for superconductivity in thin films under electric fields, including self-consistent screening. We point out connections between the dependence of electrostatic energy on superconductivity and modulation of superconductivity by fields and discuss the applicability of surface doping models in this picture. We also discuss to what degree nonlinear effects beyond linear electrostatic gating could appear in strong fields. We conclude that effects such as those observed in Ref. [15] likely are not present in the model considered. However, the results are relevant for systems with lower charge density, including epitaxial films [6–8], superconducting semiconductors [36–38], and boron-doped diamond [39].

This paper is structured as follows. In Sec. II we introduce the mean-field model considered and discuss results obtained for the electric fields and modulation of superconducting properties. Section III concludes with a discussion. The Appendixes contain auxiliary results referred to in the text.

II. MEAN-FIELD MODEL

Self-consistent electrostatic screening and the size effect on superconductivity in a clean superconducting metal in a simple mean-field approximation is convenient to consider

*Corresponding author: pauli.t.virtanen@jyu.fi

starting from a Hartree-Bogoliubov free energy. It can be obtained [34,40–42] by decoupling a long-range Coulomb and a (retarded) superconducting contact interaction via Hubbard-Stratonovich transformations and considering only the classical saddle point in the static limit:

$$\begin{aligned} F[\Delta, \phi] = & -T \operatorname{Tr} \ln \mathcal{G}^{-1} \\ & + \int d^3r \left(\rho\phi - \frac{\epsilon_0}{2}(\nabla\phi)^2 + \int_0^{\frac{1}{T}} d\tau \frac{|\Delta(\tau)|^2}{\lambda(\tau)} \right), \end{aligned} \quad (1)$$

$$\mathcal{G}^{-1} = -i\omega + \left[\frac{\hat{k}^2}{2m} - U - \mu - e\phi \right] \tau_3 + \Delta(\omega) \tau_1. \quad (2)$$

Here, \mathcal{G} is the electron equilibrium Green's function, U is a background potential, μ is a chemical potential, ϕ is equivalent to the static electric potential, Δ is the superconducting order parameter, and ρ is the ion and external charge density. The electron charge is $-e$, and we use units with $\hbar = k_B = 1$. The first term in the free energy is the electronic contribution, and the second part contains the electrostatic and superconducting mean-field contributions. In the absence of currents and magnetic field, at the saddle point and with a suitable gauge, Δ can be chosen to be real valued, and the values of the vector potential and phase are zero. Above, ϕ has to be taken as the saddle-point solution, which, as is typical for variational Poisson, does not minimize F .

Variations vs ϕ and Δ give the Poisson and BCS self-consistency equations:

$$\begin{aligned} -\epsilon_0 \nabla^2 \phi(\mathbf{r}) &= \rho(\mathbf{r}) - en_e(\mathbf{r}) \\ &= \rho(\mathbf{r}) + eT \sum_{\omega_n} \operatorname{tr} \tau_3 \mathcal{G}(\mathbf{r}, \mathbf{r}, \omega_n), \end{aligned} \quad (3)$$

$$\Delta(\mathbf{r}) = \frac{1}{2} T \sum_{|\omega_n| < \omega_c} \lambda(\mathbf{r}) \operatorname{tr} \tau_1 \mathcal{G}(\mathbf{r}, \mathbf{r}, \omega_n), \quad (4)$$

where \mathcal{G} satisfies the Gor'kov equations $\mathcal{G}^{-1}\mathcal{G} = 1$ under the self-consistent potentials. We also consider here a BCS weak-coupling model, with $\Delta(\omega) = \Delta\theta(\omega_c - |\omega|)$, with the coupling λ taken to be constant and a cutoff ω_c similar to the Debye frequency. In bulk, the BCS gap equation is then directly $\Delta = 2\omega_c e^{-1/(N_0\lambda)}$, with N_0 being the DOS per spin at the Fermi level.

For a uniform system, expanding \mathcal{G} in Eq. (3) to lowest order in ϕ results in $\epsilon^{\text{RPA}}(\mathbf{q}) q^2 \phi(\mathbf{q}) = \delta\rho(\mathbf{q})$, where $\epsilon^{\text{RPA}}(\mathbf{q}) = \epsilon_0 - \frac{\epsilon^2}{q^2} \Pi(\mathbf{q}; \Delta)$ is the self-consistent static dielectric function of a clean superconductor [43,44]. In this model, the static fields are screened, and external charge density affects the electronic DOS but not the Coulomb effect [45] on λ . The latter is due to considering the mean field with the decoupling assumed; corrections appear from fluctuations of ϕ (see, e.g., Ref. [46] for explicit calculations) or on the mean-field level with different decoupling [47].

Aiming to describe the effects on a qualitative level, we now consider a simplified model, similar to those used in several previous studies on the quantum size effect in superconducting thin films [1,3]. A confining potential $U(\mathbf{r})$ is taken to be an infinite quantum well at $|x| < L/2$, which

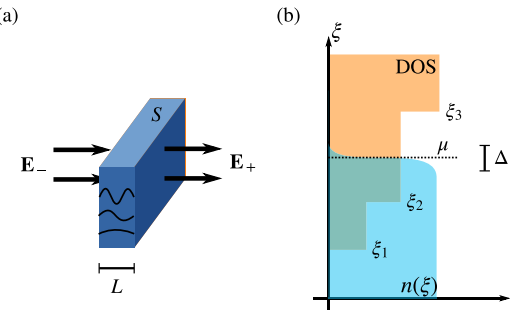


FIG. 1. (a) Schematic of superconducting quantum well of thickness L with infinite size in other directions, supporting several populated subbands, with electric fields E_{\pm} imposed on the surfaces. (b) Charge density (6) in a superconductor is determined by the density of states and an occupation factor broadened by the superconducting interaction.

supports some number of populated 2D electronic subbands (see Fig. 1). In a static problem without currents, the electric field is perpendicular to the metal surface, and the problem is inhomogeneous only in the x direction. Moreover, we take as a variational ansatz Δ , which is spatially constant [2] inside the well; the resulting energies will then be upper bounds to the exact solutions. In Appendix C we relax these assumptions and observe they retain the main physics.

With these assumptions, the problem is elementary and mostly given by known results [2,48] and can be solved without further approximations. First,

$$\mathcal{G} = - \int_{-\infty}^{\infty} d\xi A_N(\mathbf{r}, \mathbf{r}', \xi) \begin{pmatrix} \frac{u^2}{i\omega - \epsilon} + \frac{v^2}{i\omega + \epsilon} & \frac{uv}{i\omega - \epsilon} - \frac{uv}{i\omega + \epsilon} \\ \frac{uv}{i\omega - \epsilon} - \frac{uv}{i\omega + \epsilon} & \frac{v^2}{i\omega - \epsilon} + \frac{u^2}{i\omega + \epsilon} \end{pmatrix}, \quad (5)$$

where A_N is the normal-state spectral function (per spin), $u, v = [\frac{1}{2}(1 \pm \frac{\xi}{\epsilon})]^{1/2}$, and $\epsilon = \sqrt{\xi^2 + \Delta^2}$. Due to the spatial symmetry, the problem reduces to one dimension. The normal-state DOS per volume is $v(\xi) = \frac{2}{V} \int d^3r A_N(\mathbf{r}, \mathbf{r}, \xi) = \sum_{n=1}^{\infty} \frac{m}{\pi L} \theta(\xi - \xi_n)$ where ξ_n are the 2D subband edges and V is the film volume. The subbands and the potential ϕ are obtained from the Schrödinger-Poisson problem, Eq. (3), with

$$n_e[\phi] = \sum_{n=1}^{\infty} 2m|\psi_n|^2 \gamma(\xi_n), \quad (6)$$

$$\left[-\frac{1}{2m} \partial_x^2 - \mu - e\phi(x) \right] \psi_n = \xi_n \psi_n, \quad \psi_n\left(\pm\frac{L}{2}\right) = 0, \quad (7)$$

where $\psi_n(x)$ are the transverse wave functions of the 2D subbands. Here, γ describes the contribution to the charge from each subband:

$$n(\xi) = f_0(\xi) + T \sum_{|\omega| < \omega_c} \frac{\xi \Delta^2}{(\omega^2 + \xi^2 + \Delta^2)(\omega^2 + \xi^2)}, \quad (8)$$

$$\begin{aligned} \gamma(\xi) &= \int_{\xi}^{\infty} \frac{d\xi'}{2\pi} n(\xi') \xrightarrow{T \rightarrow 0} \frac{\omega_c}{4\pi^2} \ln \frac{\omega_c^2 + \xi^2 + \Delta^2}{\omega_c^2 + \xi^2} \\ &+ \frac{1}{4\pi} \left[\epsilon \frac{2}{\pi} \arctan \frac{\omega_c}{\epsilon} + |\xi| \left(1 - \frac{2}{\pi} \arctan \frac{\omega_c}{|\xi|} \right) - \xi \right], \end{aligned} \quad (9)$$

where $n(\xi) \rightarrow u^2 f_0(\epsilon) + v^2 [1 - f_0(\epsilon)]$ for $\omega_c \rightarrow \infty$ [49], f_0 is the Fermi function, and $\epsilon = \sqrt{\xi^2 + \Delta^2}$. The occupation factor n is broadened by the interactions in a window Δ around the Fermi level, with the deviation from the Fermi function starting to decay more rapidly beyond the interaction range at $|\xi| \gtrsim \omega_c$. Variations in the DOS within this window contribute to the charge response of the amplitude of superconductivity (see Fig. 1) [31,32,50].

To be specific, we assume an external charge density outside the sample (e.g., capacitor plates with constant charge density) such that the amplitudes of the electric fields at the surfaces are fixed, $-\partial_x \phi(\pm \frac{L}{2}) = E_{\pm}$. Numerically, the nonlinear Poisson problem can be solved iteratively [51] for a fixed value of Δ .

The condensation energy $f_{ns}(\Delta) = (F[\Delta, \phi_*[\Delta]] - F[0, \phi_*[0]])/\mathcal{V}$ per volume for fixed Δ now depends only on the density of states [2,48]. Via direct calculation,

$$f_{ns}(\Delta) = \frac{1}{\mathcal{V}} \int_0^\Delta d\Delta \frac{d}{d\Delta} F[\Delta, \phi_*], \quad (10)$$

where we note that $\frac{d}{d\Delta} F[\Delta, \phi_*] = \partial_\Delta F[\Delta, \phi_*]$ at the saddle point ϕ_* . Further [2],

$$f_{ns}(\Delta) = \frac{\Delta^2}{\lambda} - \int_0^\Delta d\Delta \sum_{|\omega| < \omega_c} \int_{-\infty}^\infty d\xi \frac{\nu(\xi) T \Delta}{\omega^2 + \xi^2 + \Delta^2} \quad (11)$$

$$\equiv \frac{\Delta^2}{\lambda} - \frac{m}{2\pi L} \int_0^\Delta d\Delta \Delta \sum_{n=1}^\infty g\left(\frac{\xi_n}{\Delta}\right), \quad (12)$$

$$g(y) = \frac{T}{\Delta} \sum_{|\omega| < \omega_c} \int_y^\infty dx \frac{2}{x^2 + 1 + (\omega/\Delta)^2}. \quad (13)$$

Here, $g(y) \rightarrow \int_y^\infty dx \frac{1}{\sqrt{1+x^2}} \frac{2}{\pi} \arctan \frac{\omega_c/\Delta}{\sqrt{1+x^2}}$ for $T = 0$, and further, $g(y) \rightarrow \text{arsinh}(\omega_c/\Delta) - \text{arsinh}(y)$ for $\omega_c \gg \Delta$, $T = 0$. For $T = 0$ and $\omega_c \rightarrow \infty$,

$$f_{ns}(\Delta) \approx \frac{\Delta^2}{\lambda} - \frac{m\Delta^2}{4\pi L} \sum_{\xi_n < \omega_c} [\eta(\omega_c/\Delta) - \eta(\xi_n/\Delta)], \quad (14)$$

where $\eta(y) = \text{arsinh} y + (\sqrt{y^2 + 1} - |y|)y$. The self-consistent value Δ_* is attained at a solution of $f'_{ns}(\Delta_*) = 0$.

Separating out an electrostatic contribution by subtracting the result for some reference potential ϕ_0 ,

$$\delta f_{ns} \equiv f_{ns}(\Delta; \phi_*) - f_{ns}(\Delta; \phi_0) \quad (15)$$

$$= -\frac{m}{2\pi L} \int_0^\Delta d\Delta \Delta \sum_{n=1}^\infty \left[g\left(\frac{\xi_n}{\Delta}\right) - g\left(\frac{\xi_n^{(0)}}{\Delta}\right) \right] \quad (16)$$

$$\simeq \frac{2m}{L} \sum_{n=1}^\infty \delta\gamma(\xi_n) \delta\xi_n, \quad T = 0, \omega_c \rightarrow \infty, \quad (17)$$

where $\delta\gamma(\xi) \equiv \gamma(\xi, \Delta) - \gamma(\xi, \Delta = 0)$ from Eq. (9) and $\delta\xi_n \equiv \xi_n - \xi_n^{(0)}$. The result (16) includes both gating [1,17,18] and any nonlinear effects (e.g., energy associated with quantum capacitance) in strong electric fields. Note that the above electrostatic energy contribution depends on the electric fields only via $\xi_n = \xi_n[\phi]$, an exact statement in the model here.

It is also possible to express the electrostatic energy directly in terms of the self-consistent electric field at small

field strengths. Consider an expansion of the electronic energy around a reference electric potential, considering small $\phi_1 = \phi - \phi_0$ and $\rho_1 = \rho - \rho_0$:

$$\begin{aligned} & -T \text{Tr} \ln \mathcal{G}^{-1} + T \text{Tr} \ln \mathcal{G}^{-1}|_{\phi=\phi_0} \\ &= \int d^3r (-e) n_e[\Delta, \phi_0](\mathbf{r}) \phi_1(\mathbf{r}) \\ &+ \frac{1}{2} \int d^3r d^3r' e^2 \Pi[\Delta, \phi_0](\mathbf{r}, \mathbf{r}') \phi_1(\mathbf{r}) \phi_1(\mathbf{r}') + \dots, \end{aligned} \quad (18)$$

where n_e is the electron density and Π is the density response function. Solving the resulting saddle-point equation for ϕ_1 and substituting the solution into F gives, after integration by parts,

$$f[\Delta] = f[\Delta, \phi_0] + \frac{1}{\mathcal{V}} \int d^3r \left(\rho_1 \phi_0 + \frac{1}{2} \rho_1 \phi_{1,*} \right) \quad (19)$$

$$= f[\Delta, \phi_0] + \sum_{\pm} \frac{\mp \epsilon_0 E_{\pm}}{L} \left[\phi_0 + \frac{1}{2} \phi_{1,*} \right]_{x=\pm \frac{L}{2}} + C, \quad (20)$$

$$\rho_1 = -\epsilon_0 \nabla^2 \phi_{1,*} - \int d^3r' e^2 \Pi[\Delta, \phi_0](\mathbf{r}, \mathbf{r}') \phi_{1,*}(\mathbf{r}'), \quad (21)$$

where C is independent of Δ . In this order of expansion in small ϕ_1 , the additional electrostatic field energy in (19) coincides with the standard expression. The linear term $\sim \rho_1 \phi_0$ describes a gate effect on superconductivity, which in this approach we see is related to the Δ dependence of the equilibrium potential ϕ_0 . Using Eq. (21), the quadratic part can be expressed as $\sim \phi_1 \epsilon^{\text{RPA}} \phi_1$. It corresponds to a (quantum) capacitance modulation [22,23] by superconductivity. The result (19) can be directly used for computing $\delta f_{ns}(\Delta)$ (if $\delta\phi \equiv \phi[\Delta] - \phi[0]$ is known) and is equivalent to (16) in the small-field limit. However, due to the Δ dependence of ϕ_0 it is not necessarily very practical to compute, as solving the nonlinear Poisson problem is still required. However, the above expressions can be used as a consistency check.

As noted above, we consider charge density $\rho = \rho_1 + \rho_0$, where ρ_1 outside the sample fixes the electric field at the surface. Finally, we need to specify the background (“ion”) charge density ρ_0 . The electric potential due to ρ_0 together with U gives the pseudopotential for the electron system [52]. For simplicity, unless otherwise mentioned, below we assume $\rho_0 = en_e[\Delta = 0, \phi = 0, \mu]$, which results in $\phi_0 = 0$ being the solution in the normal state and μ becoming the parameter that fixes the charge density in the normal state. This is, of course, a crude toy model of the surface electron behavior, even within Hartree-type models [28], but (see Appendix C) modifies mainly the precise positions of the subbands and not the main qualitative features of the effect of the screening of external charges on superconductivity.

A. Size effect in the electric field

In the same way as the variation in thickness [1,2], gating by a surface electric field can, in principle, make a single subband edge ξ_n cross the Fermi level, which results in a jump in superconducting properties. Such a response can be larger than in bulk material and is not captured by surface doping

models often used for the electric field effect [17,18], where the local DOS $v(x, \xi)$ is assumed to be modified in a surface layer with a thickness of a screening length λ_{TF} according to bulk relations. In addition, the field screening is not exactly Thomas-Fermi type, but this causes less relevant changes than the difference in the DOS.

The order of magnitude of δf_{ns} can be estimated in a Thomas-Fermi approximation. Taking $\phi(L/2 + x') \simeq -E\lambda_{TF}e^{x'/\lambda_{TF}}$ for $x' < 0$, $\lambda_{TF} = \sqrt{\epsilon_0/(e^2\nu_F)}$,

$$\delta\xi_n \simeq \langle n|(-e)\phi|n\rangle = \frac{\lambda_{TF}^2}{L}eE_+q(2\lambda_{TF}k_n), \quad (22)$$

where $k_n = \pi n/L$ and $q(z) = z^2/(1+z^2)$. From Eq. (17), keeping only the smallest $|\xi_n| < \omega_c$,

$$\delta f_{ns} \simeq |f_{ns,3D}| \frac{2eEa_0}{\sqrt{\xi_n^2 + \Delta^2} + |\xi_n|} \frac{\pi^2}{4(4k_F L)^2} q(2\lambda_{TF}k_n), \quad (23)$$

where $f_{ns,3D} = -\frac{1}{4}\frac{mk_F}{\pi^2}\Delta^2$ is the bulk three-dimensional (3D) condensation energy and $a_0 = 4\pi\epsilon_0/(me^2)$ is the Bohr radius. The above result is valid in the leading order in Δ , as ϕ is assumed to be independent of it. The factor $q(2\lambda_{TF}k_n)$ in reality depends on details of the screening, and below we consider it as a constant of the order of magnitude 1.

Including the next-order eigenvalue perturbation $\delta\xi_n^{(2)}$ in (16) and considering terms of order E^2 give the second-order correction,

$$\delta f_{ns}^{(2)} \simeq \frac{m}{L} \sum_{k,n=1}^{\infty} \frac{\delta\gamma(\xi_n) - \delta\gamma(\xi_k)}{\xi_n - \xi_k} |\langle k|(-e)\phi|n\rangle|^2, \quad (24)$$

where $n = k$ means the limit $\xi_k \rightarrow \xi_n$. This energy contribution is associated with the change $\Pi[\Delta, 0] - \Pi[0, 0]$ [compare Eqs. (18) and (A4)] in the static Lindhard function [43]. However, it is of the same order in Δ as the change $\Pi[0, \phi_0[\Delta]] - \Pi[0, 0]$ due to the Δ -dependent shift in the self-consistent equilibrium potential, which we have neglected in Eq. (24). As a consequence, Eq. (24) is not the only contribution to the E^2 term, and solving the self-consistent electrostatic problem is, in general, required [53]. Conversely, calculation of the effect of superconductivity on the dielectric function requires taking the self-consistency of $\Delta = \Delta_*[\phi]$ into account [44].

The overlap factor q above depends on how accurate the Thomas-Fermi screening assumption is close to the surface. For the simple problem here, we can solve the Poisson equation numerically. Such a solution is illustrated in Fig. 2(a) for $\lambda_{TF} \ll L$. Since $\lambda_{TF} \sim k_F$, screening is not fully exponential, but the electric potential exhibits $1/k_F$ oscillations. The correction $\delta\phi = \phi(\Delta) - \phi(\Delta = 0)$ to the equilibrium electrostatic potential from superconductivity is small in the high-charge-density regime considered here. The chemical potential is chosen to be close to a subband edge in Fig. 2(a).

The corresponding dependence of δf_{ns} on the electric field magnitude is shown in Fig. 2(b), where different approximations are compared with the exact result, Eq. (16) (solid line), together with the corresponding result from Eq. (23) (dotted line). The electrostatic energy expression (20) is also shown (dashed line) and coincides with the exact result in the small-field regime. Generally, the electric field effect is

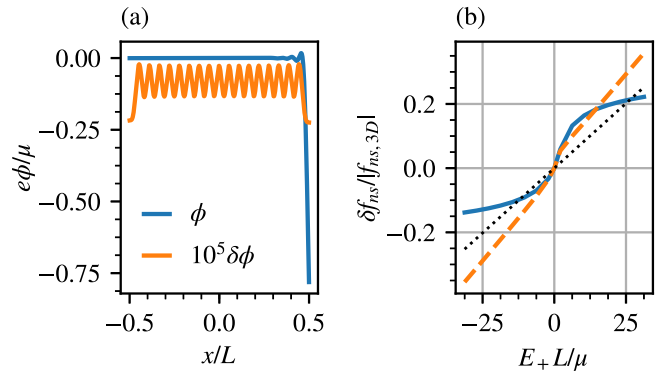


FIG. 2. (a) Self-consistent electric potential ϕ and its modulation $\delta\phi = \phi(\Delta) - \phi(\Delta = 0)$ for $E_- = 0$, $E_+ = 3.8$ V/nm, $L = 10$ nm, $\mu = \xi_{18}^{(0)} + 0.5/(mL^2) = 1.22$ eV, $\Delta = 760$ μ eV, $\omega_c = 34$ meV, $T = 0$. (b) Change δf_{ns} in the condensation energy at fixed Δ , in units of the 3D bulk condensation energy $f_{ns,3D} = -\frac{1}{4}\nu_{3D}(\mu)|\Delta|^2$. Results from Eq. (16) (solid line), the small-field expression (20) (dashed line), and Eq. (23) with $q(z) = 1$ (dotted line) are shown.

appreciable only for $E_+ L \gtrsim \mu$. In the estimate from Eq. (23), we here set $q(z) = 1$ to account for the expectation that likely, for the true screening length $\lambda_{TF}k_F \gtrsim 1$. The second-order correction (24) is negligible for these parameters, being higher order in $\lambda_{TF}^2 eE/(L\omega_c)$, and the nonlinearity visible in the result originates from $g(\xi)$.

The linear gating effect can be suppressed with a charge-neutral field configuration $E_+ = E_- = E$, which corresponds to an experiment using floating gate electrodes (i.e., placing the system inside a plate capacitor). The result from the Poisson equation for this case is shown in Fig. 3, together with the result for δf_{ns} . Imposing the field on both sides produces a larger $\delta\phi$. However, as the linear contribution to the free energy cancels, the modulation δf_{ns} arises from the next-order effect and is an order of magnitude smaller than with the gate effect. Although the energy can still be expressed via Eq. (20), the eigenvalue perturbation result (24) does not agree as well, as expected.

Whether electrostatic effects are significant depends on how large the modulation δf_{ns} is compared to f_{ns} . The

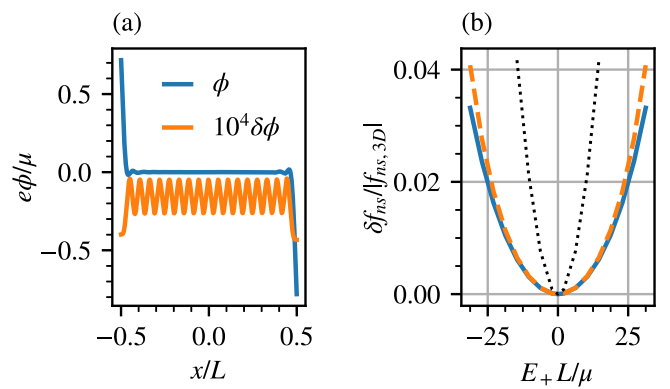


FIG. 3. Same as Fig. 2, but for the symmetric field configuration $E_+ = E_-$. The dotted line indicates Eq. (24).

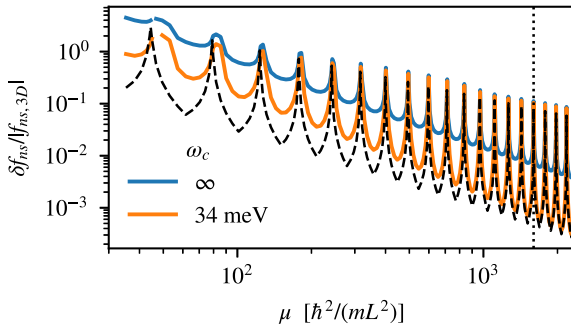


FIG. 4. Electrostatic condensation energy increase δf_{ns} vs μ for $E_+ = 0.76$ V/nm; other parameters are as in Fig. 2. The dashed line indicates Eq. (23), taking $q(z) = 1$.

dependence of their ratio on the chemical potential, and hence charge density, is shown in Fig. 4, at a relatively large external field. The magnitude of δf_{ns} depends strongly on whether the chemical potential is located near a band bottom, where the effect is amplified (see Fig. 1), which produces the oscillations visible in Fig. 4. When μ is close to a subband bottom, the magnitude appears to be captured well by Eq. (23) (dashed line). When the chemical potential is not close to a band bottom, depending on the ratio between the subband spacing and the cutoff ω_c , the electric field effect can vary by order of magnitude. Note that as long as $|\xi_n| \ll \omega_c$ for some n , the result is dominated by the smallest ξ , and the cutoff $\omega_c < \infty$ is of limited importance. The sum (16) is convergent also for $\omega_c \rightarrow \infty$. However, these results are based on the simple weak-coupling model for superconductivity, and the precise shape of the modulation may be sensitive to details of the interaction. Regardless, from the above results one can see that the relative magnitude at resonance scales as $\propto \Delta/\mu$ and not as $(\Delta/\mu)^2$ as one would expect for the amplitude response in the 3D bulk [43,44]. Away from the subband edge resonances, $\delta f_{ns} \propto (\Delta/\mu)^2$.

The self-consistent value of Δ_* , $f'_{ns}(\Delta_*) = 0$, is shown in Fig. 5(a) as a function of the film thickness, showing the well-known quantum size effect [1,2]. The corresponding dependence on the chemical potential is shown in Fig. 5(b) for several values of the external electric field. In Fig. 5(b), it is

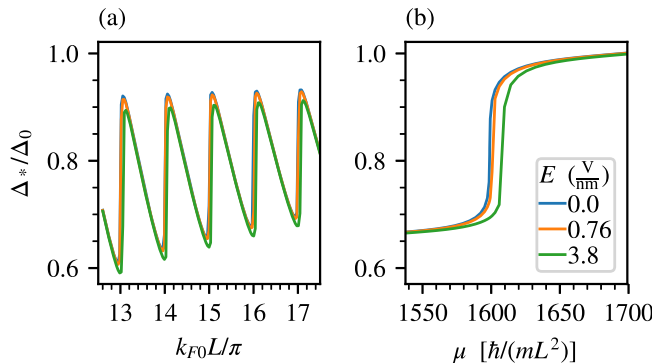


FIG. 5. Self-consistent $\Delta_*(T = 0)$ vs (a) L and (b) μ , with $g = N_{0,3D}\lambda = 0.14$ fixed and other parameters as in Fig. 2. Here, $\Delta_0 = 2\omega_c e^{-1/g}$.

obvious that the electrostatic field simply gates the system: the size effect physics is dominated by the ξ_n closest to the chemical potential, so that the gate-induced shift $\delta\xi_n$ is identical to a chemical potential shift $-\delta\mu$.

The above discussion can be compared to a surface doping model, where the DOS is assumed to change in a surface layer of thickness λ_{TF} , and the system is considered a superconducting bilayer in the Cooper limit. In such a model, $\delta F_{ns}/F_{ns} \sim -\frac{\lambda_{TF}}{L} \delta \frac{1}{v_F \lambda} \sim \frac{\delta v_F \lambda_{TF}}{\lambda v_F^2 L}$. The general form of Eq. (23) can then be recovered by including (*ad hoc*) the main features of the multiband DOS in δv_F . This can be done by writing $\frac{\delta v_F}{v_F} = \frac{\pi}{k_F L} \partial_{\xi_n} \theta_{\Delta}(\xi_n) \lambda_{TF} e E$, where $\theta_{\Delta}(\xi)$ is a broadened unit step function with width Δ . For the problem here, although the actual form of $\delta v(x, E)$ is different, this simpler model captures the main effects. Surface doping models have, indeed, been successful in understanding previous experimental results [29].

B. Superfluid weight

The effect of the electrostatic field on the phase fluctuations can be studied via the superfluid weight D_{ij}^s [54], which describes the free-energy cost of superflow $\Delta(\mathbf{r}) \propto e^{2iA \cdot \mathbf{r}}$:

$$F[\Delta_*, \phi_*, A] = F[\Delta_*, \phi_*, 0] + \frac{\hbar^2 \mathcal{V}}{2} D_{ij}^s A_i A_j + \dots \quad (25)$$

The “vector potential” A describing the superflow can be introduced in Eq. (2) by replacement $\hat{k} \mapsto \hat{k} + A$. The calculation of D^s is standard for multiband BCS superconductor. Since the current operators in the y and z directions do not couple different bands here, the result for $i, j \in \{y, z\}$ is $D_{ij}^s = \delta_{ij} \sum_n n_s(\xi_n)/(mL)$, where $n_s(\xi_n)$ is the BCS superfluid density [54]:

$$n_s(\xi) = 2m \int_{\xi}^{\infty} \frac{d\xi'}{2\pi} [n(\xi') + (\xi' - \xi) f'_0(\epsilon')], \quad (26)$$

where $n(\xi)$ is given by Eq. (8) and $\epsilon' = \sqrt{(\xi')^2 + \Delta^2}$. As is well known, $n_s(\xi) \rightarrow n_e(\xi) = 2m\gamma(\xi)$ at $T = 0$. The electrostatic modulation of the superfluid stiffness is then similar to that of the charge density, i.e., small in the metallic regime. A similar conclusion then applies to the phase stiffness and quite likely also to the phase-slip energy barrier [55]. These results, however, apply in the clean limit.

III. DISCUSSION AND CONCLUSIONS

We discussed an elementary BCS/Hartree-Bogoliubov mean-field model for the size effect under self-consistent electrostatic fields in superconducting thin films and studied it based on numerically exact solutions. As the size modulation in superconducting properties decays relatively slowly with increasing charge density, it increases the response to applied electric fields, effectively changing the small parameter from $(\Delta/\mu)^2$ to Δ/μ for fine-tuned values of μ , including in films thick compared to the screening length.

The mean-field approach likely is not useful for describing atomically thin or strongly disordered and resistive samples, where fluctuation effects matter. Phase-plasmon fluctuation effects in principle can be included in the approach above in a standard way by expanding in $\text{Re } \Delta$, $\text{Im } \Delta$, and $V = -i\phi$

around the mean-field solution. *A priori*, in view of some existing results [42,46,56], however, it is not clear why such corrections would depend strongly on the external electric field.

Large electrostatic size effects in thin-film systems are expected to be visible mainly in relatively low charge densities, e.g., semiconducting materials. As noted in previous works [29], it appears likely this is a main effect in high- T_c superconductors. The modulation of screening by superconductivity will also appear in proximity systems, e.g., in semiconductor-superconductor hybrids recently considered as Majorana fermion platforms [27,57–61]. In such nonmetallic systems with a larger ratio Δ/μ , change in the electric field configuration across the superconducting transition could be more easily observable.

With regard to the large modification of superconducting critical current by electric fields reported in Refs. [15], it then appears somewhat less likely that these results can be understood with electrostatic effects of the type discussed above. At metallic densities $\Delta/\mu \sim 10^{-4}$, electrostatic effects in the model here, even at a sharp DOS feature, likely can give only $|\delta f_{ns}/f_{ns,3D}| \lesssim 10^{-2}$, which is too small to cause large measurable effects. It appears unlikely this is easily rectified by lifting some of the approximations we made. This is simply a manifestation of the “Anderson theorem” [48]: the amplitude of conventional superconductivity is insensitive to time-reversal-symmetric perturbations, and suppressing it requires perturbations that are large compared to μ , which are usually not achievable in the metallic regime below the electrical breakdown field. Also, as the linear gate effect generally should dominate nonlinearities, whether superconductivity is suppressed or enhanced depends on the sign of the electric field, quite unlike in Ref. [15]. Finally, the observation in Sec. II B also poses some challenges to explanations via fluctuation effects, which likely would require large modulation of the stiffness without large changes in charge density. Previously, reduction in the critical current by an applied field was attributed to modification of vortex pinning [14,29]. In Ref. [15] effects appear also in aluminum strips with lateral size $\lesssim \xi$, making this explanation less favorable. In the clean-limit model here, it also appears unlikely the phase slip rates would be significantly affected.

In summary, we considered effects of electrostatic fields on superconductivity self-consistently within a BCS model, connected them to questions about electrostatic energy, and commented on their relation to recent experiments. We obtained results for the size and external electric field modulation of superconductivity and contrast results with a surface doping model. Expanding about this mean-field solution, considering electric field effects on phase slips and phase fluctuations, is possible. Experimentally, the effects are most visible in low-charge-density systems, e.g., semiconductor hybrid structures.

ACKNOWLEDGMENTS

F.G. and P.V. acknowledge the MIURFIRB2013-Project Coca (Grant No. RBFR1379UX) and the European Research Council under the European Union’s Seventh Framework Programme (FP7/2007-2013)/ERC Grant Agreement No. 615187-COMANCHE and the Horizon research and innovation program under Grant Agreement No. 800923 (SUPERTED) for partial financial support. F.G. acknowledges the innovation program under Grant No. 777222 ATTRACT (Project T-CONVERSE) and the Tuscany Region under the FARFAS 2014 project SCIADRO. A.B. acknowledges the CNR-CONICET cooperation program “Energy conversion in quantum nanoscale hybrid devices,” the SNS-WIS joint laboratory QUANTRA, funded by the Italian Ministry of Foreign Affairs and International Cooperation and the Royal Society through the international exchanges between the United Kingdom and Italy (Grants No. IES R3 170054 and No. IEC R2 192166).

vation program under Grant Agreement No. 800923 (SUPERTED) for partial financial support. F.G. acknowledges the innovation program under Grant No. 777222 ATTRACT (Project T-CONVERSE) and the Tuscany Region under the FARFAS 2014 project SCIADRO. A.B. acknowledges the CNR-CONICET cooperation program “Energy conversion in quantum nanoscale hybrid devices,” the SNS-WIS joint laboratory QUANTRA, funded by the Italian Ministry of Foreign Affairs and International Cooperation and the Royal Society through the international exchanges between the United Kingdom and Italy (Grants No. IES R3 170054 and No. IEC R2 192166).

APPENDIX A: DENSITY RESPONSE FUNCTION IN THIN FILMS

The static density response in a superconducting infinite potential well can be found in a situation translationally invariant vs y and z (i.e., response to a charge sheet). First, we have

$$\Pi(x, x') = T \sum_{\omega_n} \text{tr } \mathcal{G}(x, x') \tau_3 \mathcal{G}(x', x) \tau_3 \quad (A1)$$

$$= 2 \int_{-\infty}^{\infty} d\xi_1 d\xi_2 A_N(\mathbf{r}, \mathbf{r}'; \xi_1) A_N(\mathbf{r}, \mathbf{r}'; \xi_2)^* \times \frac{n(\xi_1, \Delta) - n(\xi_2, \Delta)}{\xi_1 - \xi_2}, \quad (A2)$$

where the trace and the Matsubara sum have been evaluated and $n(\xi) = u_\xi^2 f_0(\epsilon_\xi) + v_\xi^2 [1 - f_0(\epsilon_\xi)]$. The normal-state spectral function for a potential well is

$$A_N(x, x'; \xi) = \sum_{p=1}^{\infty} \frac{2}{L} \sin \left[k_p \left(x + \frac{L}{2} \right) \right] \times \sin \left[k_p \left(x' + \frac{L}{2} \right) \right] \delta(\xi - E_p), \quad (A3)$$

where $k_p = \frac{\pi p}{L}$, $E_p = \frac{k_p^2}{2m}$. Then we have,

$$\begin{aligned} \Pi(x, x') &= \frac{8m}{L^2} \sum_{pq=1}^{\infty} \sin \left[k_p \left(x + \frac{L}{2} \right) \right] \sin \left[k_p \left(x' + \frac{L}{2} \right) \right] \\ &\quad \times \sin \left[k_q \left(x + \frac{L}{2} \right) \right] \sin \left[k_q \left(x' + \frac{L}{2} \right) \right] \\ &\quad \times \frac{\gamma(E_p - \mu, \Delta) - \gamma(E_q - \mu, \Delta)}{E_p - E_q}, \end{aligned} \quad (A4)$$

which can be evaluated. Here, the terms $p = q$ imply the limit $E_p \rightarrow E_q$.

APPENDIX B: CONFINING POTENTIAL

In a more realistic model than in the main text, we would set $U = 0$, and the electrons would be confined in the metal film due to the attractive potential from the ionic charge density $\rho_0 > 0$. However, in such calculations the simplifying assumption of a spatially constant Δ is not permissible, as discussed below.

The charge density in a uniform 3D metal for $\mu \rightarrow -\infty$ (i.e., deep in the vacuum), with constant Δ , is

$$\begin{aligned} \rho_e(\mu, T = 0, \Delta) &= \frac{(2m)^{3/2}}{2\pi^2} \int_{-\mu}^{\infty} d\xi \sqrt{\mu + \xi} n(\xi) \\ &\simeq \frac{(2m)^{3/2}}{16\pi} \frac{\Delta^2}{\sqrt{-\mu}}. \end{aligned} \quad (\text{B1})$$

The corresponding Poisson equation in a Thomas-Fermi approximation becomes

$$\partial_x^2 \phi(x) \simeq e\epsilon_0^{-1} \rho_e(\mu - \phi(x), T = 0, \Delta) \simeq \frac{a}{\sqrt{\phi(x)}} \quad (\text{B2})$$

$$\Rightarrow \phi(x) = \left(\frac{3\sqrt{ax}}{2} \right)^{4/3}, \quad \rho_e(x) \propto x^{-2/3}. \quad (\text{B3})$$

From the solution, we find the electrostatic field fails to confine the “superconducting” electrons, and an infinite amount of total charge $\int_{x_0}^{\infty} dx \rho_e(x)$ leaks to the vacuum, which is unphysical. In the exact solution, the mean field $|\Delta(\mathbf{r})|$ would decrease simultaneously with the density, providing a stronger electrostatic confinement. Although the details of this surface effect appear sensitive to the external electric field, it appears unlikely it is important for the stability of superconductivity in the bulk.

APPENDIX C: SPATIAL DEPENDENCE OF Δ

In the main text, we take the approximation $\Delta(\mathbf{r}) = \Delta_0$ for the superconducting order parameter. In this section, we relax this assumption.

Writing the problem in the wave function basis (7), we have

$$(\mathcal{G}^{-1})_{pq} = [-i\omega + (\xi_p + \xi_{\perp})\tau_3]\delta_{pq} + \Delta_{pq}\tau_1, \quad (\text{C1})$$

$$\Delta_{pq} = \int dx \psi_p(x)\psi_q(x)\Delta(x), \quad (\text{C2})$$

where $\xi_{\perp} = \frac{k_{\perp}^2}{2m}$ and k_{\perp} is the momentum component perpendicular to x . The spatially inhomogeneous order parameter induces effectively a mixing term Δ_{pq} between different bands, resulting in equations similar to a multiband superconductor. Note that in the absence of supercurrent or external magnetic field $\Delta_{pq} = \Delta_{qp}$. Both ξ_p and Δ_{pq} depend on the electrostatic potential ϕ . The self-consistency equation becomes [4,62]

$$\Delta_{pq} = \sum_{rs} V_{pq,rs} \mathcal{F}_{rs}, \quad (\text{C3})$$

$$\mathcal{F}_{rs} = \int_0^{\infty} \frac{md\xi_{\perp}}{2\pi} \frac{T}{2} \sum_{|\omega_n| < \omega_c} \text{tr } \tau_1 \mathcal{G}_{rs}, \quad (\text{C4})$$

$$V_{pq,rs} = \int_{-\infty}^{\infty} dx \lambda(x) \psi_p(x) \psi_q(x) \psi_r(x) \psi_s(x), \quad (\text{C5})$$

and the charge density is

$$n_e(x) = \sum_{pq=1}^{\infty} 2m \psi_p(x) \psi_q(x) \gamma_{pq}, \quad \gamma_{pq} = \int_0^{\infty} \frac{d\xi_{\perp}}{2\pi} n_{pq}, \quad (\text{C6})$$

$$n_{pq} = f_0(\xi_p + \xi_{\perp})\delta_{pq} + \frac{T}{2} \sum_{|\omega_n| < \omega_c} \text{tr } \tau_3 [\mathcal{G}_{pq}|_{\Delta=0} - \mathcal{G}_{pq}]. \quad (\text{C7})$$

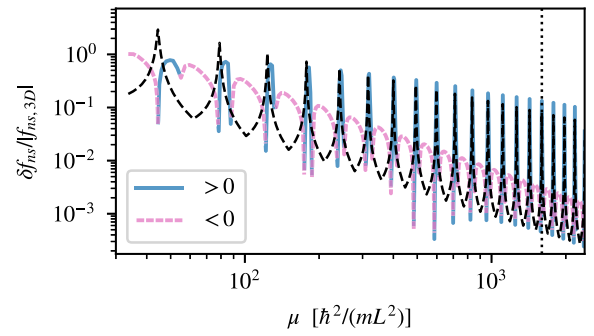


FIG. 6. Same as Fig. 4, but computed self-consistently from Eq. (C8) within the multiband approximation. To make a comparison to Fig. 4, we set here $\omega_c = 34$ meV and $\lambda(\mu)$, such that $\Delta_0 = 2\omega_c e^{-1/[N_{0,3D}(\mu)\lambda(\mu)]} = 760$ μ eV. The absolute value $|\delta f_{ns}|$ is plotted, with negative regions indicated with a different line style.

The condensation energy can be found via variation of the coupling constant, $\lambda \mapsto \lambda\chi$, and

$$f_{ns} = - \int_0^1 d\chi \int d^3r \frac{(\Delta^{\chi})^2}{\mathcal{V}\lambda\chi^2} = -\frac{1}{L} \int_0^1 \frac{d\chi}{\chi} \sum_{rs} \Delta_{rs}^{\chi} \mathcal{F}_{rs}^{\chi}, \quad (\text{C8})$$

where Δ^{χ} , ϕ^{χ} , and \mathcal{F}^{χ} are the values computed self-consistently for fixed χ . The discussion in the main text corresponds to taking $\Delta_{pq} = \Delta_0 \delta_{pq}$ in the above. We again define the electrostatic component $\delta f_{ns} = f_{ns} - f_{ns}|_{E_+ = E_- = 0}$ as the modulation due to the external field.

The problem retains a form similar to that in the main text if subband off-diagonal matrix elements are dropped on the right-hand sides of the above equations (Anderson approximation), taking $\mathcal{G}_{pq}^{-1} \propto \delta_{pq}$ [62]. Then, $\gamma_{pq} = \delta_{pq}\gamma(\xi_p)|_{\Delta=\Delta_{pp}}$ is given by Eq. (9), and $\mathcal{F}_{rs} = \delta_{rs}[m\Delta/(4\pi)]g(\xi_r/\Delta)|_{\Delta=\Delta_{rr}}$ is given by Eq. (13). For uniform $\lambda(x) = \lambda_0$ inside the film, $V_{pp,qq} \simeq (1 + \frac{1}{2}\delta_{pq})\frac{\lambda_0}{L}$, up to electric field corrections. With such all-to-all coupling and a large number $N \gg 1$ of bands in the regime we are interested in, the self-consistent problem remains qualitatively close to that discussed in the main text. The electrostatic free-energy contribution within this approximation is shown in Fig. 6. The result remains quantitatively similar to Fig. 4 close to resonances and agrees in order of magnitude away from them. The results also show an additional change in the sign of the electrostatic

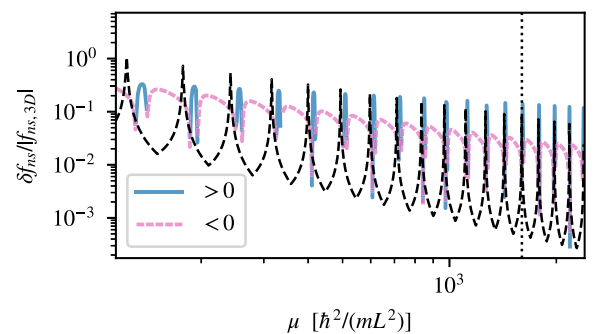


FIG. 7. Same as Fig. 6, but with $U = 0$ and only electrostatic confinement, assuming positive ion charge density $\rho_0 = e(2m\mu)^{3/2}/(3\pi^2\hbar^3)$ in the region $|x| < L/2$.

energy contribution in the regime where the effect is smallest and the physics is not dominated by a single band and is more sensitive to details of the interaction. In these parameter regions, the effect of a strong electric field is not only a simple shift in the effective chemical potential.

This approximation also avoids the issue discussed in Appendix B, and we can consider $U = 0$ and only elec-

trostatic confinement. The result is shown in Fig. 7. It remains qualitatively similar to Figs. 4 and 6, but with a small shift in the band bottom positions, as expected for a finite potential well; changes in the normal-state screening factor $q(2\lambda_{TF}k_n) \simeq \delta\xi_n L / (\lambda_{TF}^2 e E_+)$; and a larger $|\delta f_{ns}|$ in the parameter regions between the band bottoms.

-
- [1] J. M. Blatt and C. J. Thompson, *Phys. Rev. Lett.* **10**, 332 (1963).
- [2] D. S. Falk, *Phys. Rev.* **132**, 1576 (1963).
- [3] A. A. Shanenko, M. D. Croitoru, and F. M. Peeters, *Phys. Rev. B* **75**, 014519 (2007).
- [4] A. A. Shanenko, J. A. Aguiar, A. Vagov, M. D. Croitoru, and M. V. Milošević, *Supercond. Sci. Technol.* **28**, 054001 (2015).
- [5] B. G. Orr, H. M. Jaeger, and A. M. Goldman, *Phys. Rev. Lett.* **53**, 2046 (1984).
- [6] Y. Guo, Y.-F. Zhang, X.-Y. Bao, T.-Z. Han, Z. Tang, L.-X. Zhang, W.-G. Zhu, E. G. Wang, Q. Niu, Z. Q. Qiu, J.-F. Jia, Z.-X. Zhao, and Q.-K. Xue, *Science* **306**, 1915 (2004).
- [7] Y.-F. Zhang, J.-F. Jia, T.-Z. Han, Z. Tang, Q.-T. Shen, Y. Guo, Z. Q. Qiu, and Q.-K. Xue, *Phys. Rev. Lett.* **95**, 096802 (2005).
- [8] X.-Y. Bao, Y.-F. Zhang, Y. Wang, J.-F. Jia, Q.-K. Xue, X. C. Xie, and Z.-X. Zhao, *Phys. Rev. Lett.* **95**, 247005 (2005).
- [9] J. Mannhart, *Mod. Phys. Lett. B* **06**, 555 (1992).
- [10] J. Mannhart, J. G. Bednorz, K. A. Müller, D. G. Schlom, and J. Ströbel, *J. Alloys Compd.* **195**, 519 (1993).
- [11] C. H. Ahn, J.-M. Triscone, and J. Mannhart, *Nature (London)* **424**, 1015 (2003).
- [12] D. Matthey, N. Reyren, J. M. Triscone, and T. Schneider, *Phys. Rev. Lett.* **98**, 057002 (2007).
- [13] C. H. Ahn, A. Bhattacharya, M. Di Ventra, J. N. Eckstein, C. D. Frisbie, M. E. Gershenson, A. M. Goldman, I. H. Inoue, J. Mannhart, A. J. Millis, A. F. Morpurgo, D. Natelson, and J.-M. Triscone, *Rev. Mod. Phys.* **78**, 1185 (2006).
- [14] D. Shvarts, M. Hazani, B. Y. Shapiro, G. Leitus, V. Sidorov, and R. Naaman, *Europhys. Lett.* **72**, 465 (2005).
- [15] G. De Simoni, F. Paolucci, P. Solinas, E. Strambini, and F. Giazotto, *Nat. Nanotechnol.* **13**, 802 (2018); F. Paolucci, G. De Simoni, E. Strambini, P. Solinas, and F. Giazotto, *Nano Lett.* **18**, 4195 (2018); F. Paolucci, G. De Simoni, P. Solinas, E. Strambini, N. Ligato, P. Virtanen, A. Braggio, and F. Giazotto, *Phys. Rev. Appl.* **11**, 024061 (2019).
- [16] P. Lipavský, J. Koláček, K. Morawetz, and E. H. Brandt, *Phys. Rev. B* **65**, 144511 (2002).
- [17] B. Y. Shapiro, *Phys. Lett. A* **105**, 374 (1984).
- [18] B. Y. Shapiro, *Solid State Commun.* **53**, 673 (1985).
- [19] W. D. Lee, J. L. Chen, T. J. Yang, and B.-S. Chiou, *Phys. C (Amsterdam, Neth.)* **261**, 167 (1996).
- [20] L. Burlachkov, I. B. Khalfin, and B. Y. Shapiro, *Phys. Rev. B* **48**, 1156 (1993).
- [21] P. Lipavský, K. Morawetz, J. Koláček, and T. J. Yang, *Phys. Rev. B* **73**, 052505 (2006).
- [22] K. Morawetz, P. Lipavský, J. Koláček, and E. H. Brandt, *Phys. Rev. B* **78**, 054525 (2008).
- [23] K. Morawetz, P. Lipavský, and J. J. Mareš, *New J. Phys.* **11**, 023032 (2009).
- [24] G. A. Ummarino, E. Piatti, D. Daghero, R. S. Gonnelli, I. Y. Sklyadneva, E. V. Chulkov, and R. Heid, *Phys. Rev. B* **96**, 064509 (2017).
- [25] T. Koyama, *J. Phys. Soc. Jpn.* **70**, 2102 (2001).
- [26] M. Machida and T. Koyama, *Phys. Rev. Lett.* **90**, 077003 (2003).
- [27] B. D. Woods, T. D. Stanescu, and S. Das Sarma, *Phys. Rev. B* **98**, 035428 (2018).
- [28] N. D. Lang and W. Kohn, *Phys. Rev. B* **1**, 4555 (1970).
- [29] J. Mannhart, D. G. Schlom, J. G. Bednorz, and K. A. Müller, *Phys. Rev. Lett.* **67**, 2099 (1991).
- [30] J. W. Gadzuk and E. W. Plummer, *Rev. Mod. Phys.* **45**, 487 (1973).
- [31] C. J. Adkins and J. R. Waldram, *Phys. Rev. Lett.* **21**, 76 (1968).
- [32] D. I. Khomskii and F. V. Kusmartsev, *Phys. Rev. B* **46**, 14245 (1992).
- [33] D. I. Khomskii and A. Freimuth, *Phys. Rev. Lett.* **75**, 1384 (1995).
- [34] A. van Otterlo, M. Feigel'man, V. Geshkenbein, and G. Blatter, *Phys. Rev. Lett.* **75**, 3736 (1995).
- [35] D. Belitz and T. R. Kirkpatrick, *Rev. Mod. Phys.* **66**, 261 (1994).
- [36] J. F. Schooley, W. R. Hosler, and M. L. Cohen, *Phys. Rev. Lett.* **12**, 474 (1964).
- [37] J. F. Schooley, W. R. Hosler, E. Ambler, J. H. Becker, M. L. Cohen, and C. S. Koonce, *Phys. Rev. Lett.* **14**, 305 (1965).
- [38] E. Bustarret, C. Marcenat, P. Achatz, J. Kačmarčík, F. Lévy, A. Huxley, L. Ortéga, E. Bourgeois, X. Blase, D. Débarre, and J. Boulmer, *Nature (London)* **444**, 465 (2006).
- [39] E. A. Ekimov, V. A. Sidorov, E. D. Bauer, N. N. Mel'nik, N. J. Curro, J. D. Thompson, and S. M. Stishov, *Nature (London)* **428**, 542 (2004).
- [40] T. M. Rice, *J. Math. Phys.* **8**, 1581 (1967).
- [41] V. Ambegaokar, U. Eckern, and G. Schön, *Phys. Rev. Lett.* **48**, 1745 (1982).
- [42] A. van Otterlo, D. S. Golubev, A. D. Zaikin, and G. Blatter, *Eur. Phys. J. B* **10**, 131 (1999).
- [43] R. E. Prange, *Phys. Rev.* **129**, 2495 (1963).
- [44] J. Seiden, *J. Phys. France* **27**, 561 (1966).
- [45] P. Morel and P. W. Anderson, *Phys. Rev.* **125**, 1263 (1962).
- [46] S. Fischer, M. Hecker, M. Hoyer, and J. Schmalian, *Phys. Rev. B* **97**, 054510 (2018).
- [47] H. J. Schulz, *Phys. Rev. Lett.* **65**, 2462 (1990).
- [48] P. W. Anderson, *J. Phys. Chem. Solids* **11**, 26 (1959).
- [49] M. Tinkham, *Introduction to Superconductivity*, 2nd ed. (McGraw-Hill, New York, 1996).
- [50] K. M. Hong, *Phys. Rev. B* **12**, 1766 (1975).
- [51] V. Eyert, *J. Comput. Phys.* **124**, 271 (1996).

- [52] The confining potential U is not necessary for the formulation, except for enabling the use of the constant- Δ approximation; see Appendixes B and C.
- [53] Alternatively, one could base the expansion (18) around the normal-state potential $\phi_0 = 0$ and include a third-order term $\int \Gamma_3(x, x', x'')\phi(x)\phi(x')\phi(x'')$.
- [54] D. J. Scalapino, S. R. White, and S. Zhang, *Phys. Rev. B* **47**, 7995 (1993).
- [55] J. S. Langer and V. Ambegaokar, *Phys. Rev.* **164**, 498 (1967).
- [56] K. Y. Arutyunov, D. S. Golubev, and A. D. Zaikin, *Phys. Rep.* **464**, 1 (2008).
- [57] Y. Oreg, G. Refael, and F. von Oppen, *Phys. Rev. Lett.* **105**, 177002 (2010).
- [58] A. Vuik, D. Eeltink, A. R. Akhmerov, and M. Wimmer, *New J. Phys.* **18**, 033013 (2016).
- [59] M. Hell, M. Leijnse, and K. Flensberg, *Phys. Rev. Lett.* **118**, 107701 (2017).
- [60] F. Pientka, A. Keselman, E. Berg, A. Yacoby, A. Stern, and B. I. Halperin, *Phys. Rev. X* **7**, 021032 (2017).
- [61] P. Virtanen, F. S. Bergeret, E. Strambini, F. Giavotto, and A. Braggio, *Phys. Rev. B* **98**, 020501(R) (2018).
- [62] Y. Chen, A. A. Shanenko, and F. M. Peeters, *Phys. Rev. B* **85**, 224517 (2012).